UCRL-PROC-206274

LAWRENCE
LIVERMORE
NATIONAL
LABORATORY

Large-Actuator-Number Horizontal Path Correction of Atmospheric Turbulence utilizing an Interferometric Phase Conjugate Engine

K. L. Baker, E. A. Stappaerts, D. Gavel, J. Tucker, D. A. Silva, S. C. Wilks, S. S. Olivier, J. Olsen

August 27, 2004

AMOS Conference 2004
Wailea, Maui, HI, United States
September 13, 2004 through September 17, 2004

Disclaimer

Large-Actuator-Number Horizontal Path Correction of Atmospheric Turbulence utilizing an Interferometric Phase Conjugate Engine

K.L. Baker, E.A. Stappaerts, D. Gavel, J. Tucker, D.A. Silva, S.C. Wilks, S.S. Olivier, J. Olsen

Lawrence Livermore National Laboratory, Livermore, CA, USA

Abstract

An adaptive optical system used to correct horizontal beam propagation paths has been demonstrated. This system utilizes an interferometric wave-front sensor and a large-actuator-number MEMS-based spatial light modulator to correct the aberrations incurred by the beam after propagation along the path. Horizontal path correction presents a severe challenge to adaptive optics systems due to the short atmospheric transverse coherence length and the high degree of scintillation incurred by laser propagation along these paths. Unlike wave-front sensors that detect phase gradients, however, the interferometric wave-front sensor measures the wrapped phase directly. Because the system operates with nearly monochromatic light and uses a segmented spatial light modulator, it does not require that the phase be unwrapped to provide a correction and it also does not require a global reconstruction of the wave-front to determine the phase as required by gradient detecting wave-front sensors. As a result, issues with branch points are eliminated. Because the atmospheric probe beam is mixed with a large amplitude reference beam, it can be made to operate in a photon noise limited regime making its performance relatively unaffected by scintillation. The MEMS-based spatial light modulator in the system contains 1024 pixels and is controlled to speeds in excess of 800 Hz, enabling its use for correction of horizontal path beam propagation. In this article results are shown of both atmospheric characterization with the system and open loop horizontal path correction of a 1.53 micron laser by the system. To date Strehl ratios of greater than 0.5 have been achieved.

I. INTRODUCTION

Adaptive optics (AO) systems used in astronomy and vision applications typically utilize Shack-Hartmann wave-front sensors [1,2]. These sensors measure the gradient of the phase and commonly utilize least squares phase reconstruction algorithms. When coherent light propagates over atmospheric paths, the beam develops large intensity fluctuations and phase residues [3], severely degrading the performance of these wave-front sensors. Recently, a prototype of the coherent light AO system described in this article was demonstrated using a visible laser and a liquid crystal spatial light modulator (SLM) [4]. It allowed many concept features to be tested, but its speed was limited to ~1 Hz due to the SLM response time. This article discusses a coherent light AO system based on a quadrature Twyman-Green interferometer operating at a wavelength of 1.5 μm and at speeds in excess of 800 Hz through atmospheric turbulence [5,6]. The technique mixes an atmospheric probe beam with a large amplitude reference beam, allowing it to operate in a photon-noise limited regime even in the case of large scintillation. It does not require a global reconstruction of the phase, making it much less sensitive to phase residues. These attributes make this approach to phase conjugation much more robust than conventional AO systems employing Shack-Hartmann wave-front sensors for applications involving coherent light propagation through strong turbulence.

In section II, the experimental layout of the phase conjugate engine is presented along with a description of its operation. Section III details the experimental characterization and operation of the system in a field test with atmospheric turbulence. These results are then summarized in the IV and final section.

II. EXPERIMENTAL LAYOUT

The optical layout of the IR system is shown in Fig. 1. It consists primarily of an interferometric wave-front sensor, a MEMS-based spatial-light-modulator built by the Boston Micromachines Corporation (BMC), an Erbium-doped fiber laser built by HRL laboratories and computer hardware/software to analyze the wave-front and implement the phase correction. The system was designed for open-loop operation, however, a closed-loop arm exists such that the wave-front camera can be aligned precisely with the MEMS-based spatial light modulator and either configuration can be used simply by blocking the remaining beam path. The laser source is an Erbium-doped fiber laser operating at 1530 nm. The laser has two independently triggerable arms, which output nearly transform-limited pulses of 1 ns duration and pulse energies of 7 μJ and 100 nJ for the probe beam and the reference beam, respectively.

Polarization components are utilized in the system to form the two interferograms with a $\pi/2$ phase shift between them and also to control the relative signal levels in the arms of the interferometer. The reference beam passes through a quarter wave-plate converting the linearly polarized light into circularly polarized light. The reference beam is mixed with the probe beam after the probe beam has traversed the aberrating medium, atmosphere or Kolmogorov phase screens, and passed through a half wave-plate to rotate the polarization such that equal components of horizontal and vertical fields in the probe beam are combined with the circularly polarized reference beam. A Wollaston prism is then used to angularly separate the horizontal and vertical polarizations of the reference and probe beams into the two interferograms with a $\pi/2$ phase shift between the reference beams in the two separate interferograms.

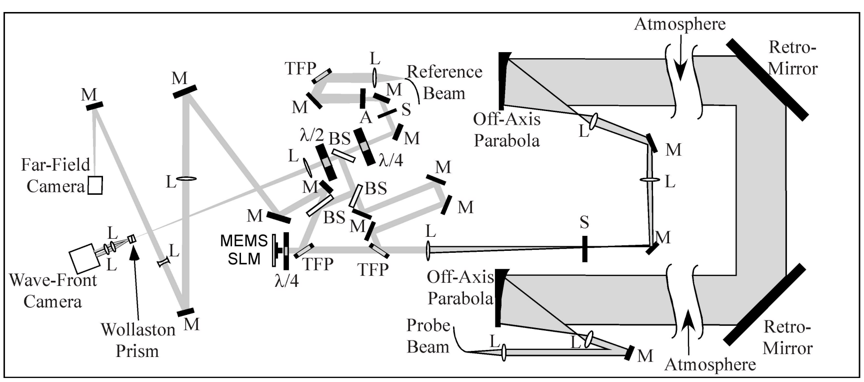

Figure 1 Field test setup used to test the performance of the phase conjugate engine over an atmospheric propagation path. The abbreviations stand for the following: BS, beam splitters; M, mirrors; L, lenses; S, shutters; A, apertures; TFP, thin film polarizers; $\lambda/2$ and λ /4, half and quarter wave-plates, respectively.

III. FIELD TEST EXPERIMENTAL RESULTS

The topology of the field test site was defined by rolling hills. The experiment was carried out across a valley between two of these hills, one of which contained the AO system and the other a 2-mirror retro-reflector. The AO system was slightly higher in elevation than the retro-reflector, with an approximate drop in elevation of 100 meters to the valley floor between the two hills. The roundtrip distance traveled by the probe beam was approximately 1.35 km, for a transit time of approximately 4.5 μs.

The turbulence over the propagation path was characterized by measuring the aberrated phase profile of the probe beam after passing through the atmosphere. A large number of interferograms, ~3000, were acquired at a frequency of ~580 Hz. These interferograms contained the information required to determine the two-dimensional, wrapped (modulo-2π), phase across the input aperture of the system. Before the parameters used to describe the turbulence spectrum could be determined, the phase had to be unwrapped. The phase was unwrapped using a minimum weighted discontinuity method [7]. This technique partitions the wrapped phase profile into two connected regions, separated by discontinuity curves. The algorithm then raises the phase in one of the regions by 2π, thereby reducing the weighted sum of the discontinuities. This process is repeated until no further partitioning is possible. Once the unwrapped phase has been recovered, the parameters and scaling relations used to describe the turbulence spectrum can be determined. One such scaling relation is the phase structure function, $D_\phi(r)$. The phase structure function is defined by $D_\phi(r) = \langle|\phi(x)-\phi(x+r)|^2\rangle$, which for a Kolmogorov turbulence spectrum can be expressed analytically as $D_\phi(r) = 6.88(r/r_o)^{5/3}$, in the limit $r \gg (\lambda L)^{0.5}$. In this expression, r_o is the Fried parameter or transverse coherence length and λ and L are the wavelength and propagation length, respectively [8]. The phase structure function is constructed by comparing the phase at a given location to the phase at an increasing distance from that location. A median average over 3000 such structure functions is shown in Fig. 2. There is a good fit between the slopes of the averaged, experimentally determined, function and the analytic form for a Kolmogorov turbulence spectrum. The solid black line represents the data, the solid gray line represents the Kolmogorov fit for a Fried parameter of 2.4 cm and the two dashed black lines represent Kolmogorov fits for Fried parameters of 2.0 cm and 3.0 cm, respectively.

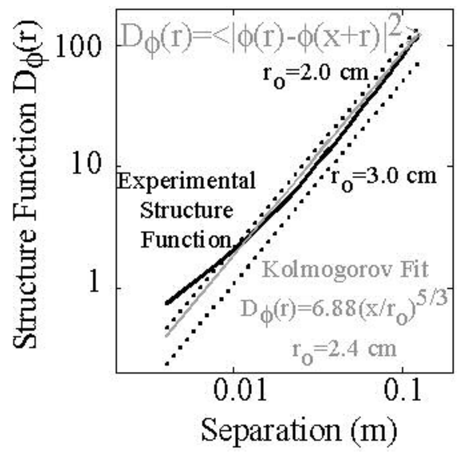

Figure 2 Phase structure function averaged over 3000 measured functions, which were calculated by unwrapping the wrapped phases determined from 3000 sets of sine and cosine interferograms.

The performance of the AO system was again quantified by measuring the Strehl ratio. The Strehl ratio was calculated by measuring both the point-spread-function (PSF), with a far-field camera, and the near-field image of the probe beam, with the wave-front camera. The near field images were collected at a slightly delayed time by blocking the reference beam. Fig. 3 shows the PSF for the uncorrected probe beam, Fig. 3a, and the corrected probe beam, Fig. 3b. With these two measurements, the Strehl ratio was calculated and compared with the expected phase variance associated with a Kolmogorov turbulence spectrum. A sequence of 100 PSFs was taken and the absolute instantaneous Strehl ratios determined from these measurements, with the system on and off, as shown in Fig. 4. The instantaneous Strehl ratios were averaged over the 100 frames to quantify the system performance. The figure indicates an average corrected Strehl ratio of S_r=0.46, a tip/tilt only Strehl ratio of S_r=0.19 and a Strehl ratio of S_r=0.06 without tip/tilt correction. The uncorrected value, S_r=0.06, is in reasonably good agreement with the expected value of $S_r=(r_o/D)^2=(2.4\text{ cm}/13\text{ cm})^2=0.03$.

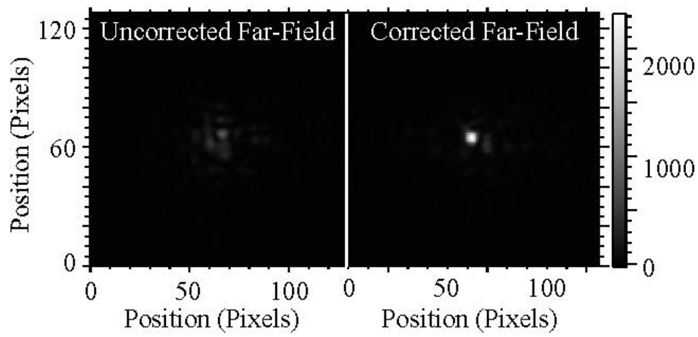

Figure 3 Point-spread-functions for the uncorrected and correct probe beams after propagation through the atmosphere.

An estimate of the Strehl ratio with the system on was made as follows. The ratio due to the fitting error, for a Kolmogorov turbulence spectrum and a square aperture, is given by $S_r=\exp\{-1.3(d/r_o)^{5/3}\}$, where d is the sub-aperture size [9]. For the field test, the sub-aperture size was approximately 4 mm, yielding an expected Strehl ratio of Sr ~ 0.94.. The MEMS-based spatial light modulator, which consisted of 32x32 pixels, in the phase conjugate engine had approximately 60 bad pixels and the outer actuators were not activated giving nearly 18% of the actuators that were not contributing to the correction. Wave optics simulations performed using a bad pixel map of the actuators indicated that the non-activated pixels caused a reduction in the Strehl ratio of approximately 22 %. This gave an estimated maximum achievable Strehl ratio of $S_r=(1.0-0.22)\exp\{-1.3(d/r_o)^{5/3}\}\sim0.73$. Given the wind velocities and system operating speed~~s~~, the effects of time delay error were negligible. The achievable Strehl ratio is further reduced by the 3-bit algorithm [10,11] used to determine the phase, lowering it by a factor of 0.95 to $S_r\sim0.95*0.73 = 0.69$. The measured value of 0.46 is then within approximately 40 % of the maximum achievable Strehl ratio. The discrepancy is likely due to slight registration errors, camera gain nonlinearities and small errors in calibration of the SLM response curves.

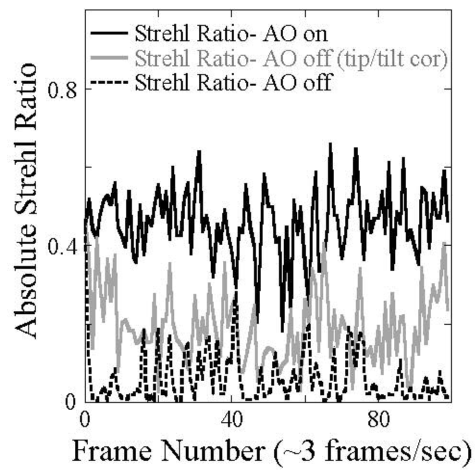

Figure 4 Absolute Strehl ratios as a function of time. The solid black line represents the Strehl ratio with the AO system turned on, while the dashed black line represents the Strehl ratio with the system turned off. The solid gray line represents the Strehl ratio with the system turned off but with the center of mass of the point spread function moved to the central axis, as would occur if a tip/tilt system were running.

IV. SUMMARY

In the field test the AO system achieved large improvements, ~8x, over the uncorrected PSF for the 1.35 km atmospheric propagation path. The system successfully demonstrated the use of a large actuator number, 1024, MEMS-based SLM at speeds in excess of 800 Hz. This work demonstrates the potential of such SLMs to replace conventional deformable mirrors for applications requiring high Strehl ratios such as multi-conjugate and extreme AO systems, AO systems for extremely large telescopes and communications and imaging under conditions of strong turbulence.

Acknowledgements

The authors would like to acknowledge a number of contributors to this project. M.L. Minden and Hughes Research Laboratories provided the Erbium-doped fiber laser used in these experiments. P. Bierden and the Boston Research Corporation provided the MEMS-based spatial light modulator. The authors would also like to acknowledge discussions with W.H Long, Jr. regarding simulations of the expected performance of the system in various applications, H. Komine for suggesting a Wollaston prism, in the configuration shown in Fig. 1, for channel separation on the CCD camera and L.G. Seppala for contributions to the optical design. This effort was sponsored by the Defense Advanced Research Projects Agency (DARPA) for work on the Coherent Communications, Imaging and Targeting (CCIT) program, 02-L493. This work was performed under the auspices of the U.S. Department of Energy by the University of California, Lawrence Livermore National Laboratory under contract No. W-7405-Eng-48.

REFERENCES

[1] J. W. Hardy, *Adaptive Optics for Astronomical Telescopes* (Oxford University Press, Oxford, 1998).

[2] R. K. Tyson, *Principles of Adaptive Optics* (Academic Press, Boston, 1998).

3 David L. Fried, “Branch point problem in adaptive optics,” J. Opt. Soc. Am. A **15** (10), 2759 (1998).

4 K. L. Baker, E. A. Stappaerts, S. C. Wilks, P.E. Young, D. Gavel, J. Tucker, D.A. Silva and S.S. Olivier, “Open and Closed-Loop Aberration Correction using a Quadrature Interferometric Wave-Front Sensor,” Opt. Lett. **29**, 47 (2004).

5 K.L. Baker, E.A. Stappaerts, D. Gavel, S.C. Wilks, J. Tucker, D.A. Silva, J. Olsen, S.S. Olivier, P.E. Young, M.W. Kartz, L.M. Flath, P. Kruelevitch, J. Crawford and Oscar Azucena, “High-speed horizontal-path atmospheric turbulence correction using a large actuator-number MEMS spatial light modulator in an interferometric phase conjugation engine,” accepted by Opt. Lett.

6 K.L. Baker, E.A. Stappaerts, D. Gavel, S.C. Wilks, J. Tucker, D.A. Silva, J. Olsen, S.S. Olivier, P.E. Young, M.W. Kartz, L.M. Flath, P. Kruelevitch, J. Crawford and Oscar Azucena, "Breadboard Testing of a Phase Conjugate Engine with an Interferometric Wave-Front Sensor and a MEMS-Based Spatial Light Modulator," accepted by Appl. Opt.

7 T. J. Flynn, "Two-dimensional phase unwrapping with minimum weighted discontinuity," JOSA A **14**, 2692 (1997).

8 D.L. Fried "Optical resolution through a randomly inhomogeneous medium for very long and very short exposures," JOSA Vol.56 No.10 pp1372-1379 (1966).

9 R. Hudgin, "Wave-front compensation error due to finite corrector-element size," JOSA Vol.67 No.3, pp393-395 (1977).

10 Gordon D. Love, Nigel Andrews, Philip Burch, David Buscher, Peter Doel, Colin Dunlop, John Major, Richard Myers, Alan Purvis, Ray Sharples, Andrew Vick, Andrew Zadrozny, Sergio R. Restaino and Andreas Glindemann, "Binary adaptive optics: atmospheric wave-front correction with a half-wave phase shifter," Applied Optics **34**, 6058 (1995).

11 K. L. Baker, E. A. Stappaerts, S. C. Wilks, D. Gavel, P.E. Young, J. Tucker, D.A. Silva, S.S. Olivier and J. Olsen, "Performance of a phase-conjugate-engine implementing a finite-bit phase correction," Opt. Lett. **29**, pp980-982 (2004).